MedChemComm

Accepted Manuscript

ROYAL SOCIETY OF CHEMISTRY

www.rsc.org/medchemcomm

Cite this: DOI: 10.1039/c0xx00000x

www.rsc.org/xxxxxx

ARTICLE TYPE

Synthesis and anti-cancer screening of novel heterocyclic-(2*H*)-1,2,3-triazoles as potential anti-cancer agents

Narsimha Reddy Penthala,[a] Leena Madhukuri,[b] Shraddha Thakkar,[a] Nikhil Reddy Madadi,[a] Gauri Lamture,[a] Robert L. Eoff[b] and Peter A. Crooks[a]*

Received (in XXX, XXX) Xth XXXXXXXXX 20XX, Accepted Xth XXXXXXXXX 20XX
DOI: 10.1039/b000000x

trans-Cyanocombretastatin A-4 (*trans*-CA-4) analogues have been structurally modified to afford their more stable CA-4-(2*H*)-1,2,3-triazole analogues. Fifteen novel, stable 4-heteroaryl-5-aryl-(2*H*)-1,2,3-triazole CA-4 analogues (**8a-i**, **9** and **11a-e**) were evaluated for anti-cancer activity against a panel of 60 human cancer cell lines. These analogues displayed potent cytotoxic activity against both hematological and solid tumor cell lines with GI_{50} values in the low nanomolar range. The most potent compound, **8a**, was a benzothiophen-2-yl analogue that incorporated a 3,4,5-trimethoxyphenyl moiety connected to the (2*H*)-1,2,3-triazole ring system. Compound **8a** exhibited GI_{50} values of <10 nM against 80% of the cancer cell lines in panel. Three triazole analogues, **8a**, **8b** and **8g**, showed particularly potent growth inhibition against the triple negative Hs578T breast cancer cell line with GI_{50} values of 10.3 nM, 66.5 nM and 20.3 nM, respectively. Molecular docking studies suggest that these compounds bind to the same hydrophobic pocket at the interface of α- and β-tubulin that is occupied by colchicine and *cis*-CA-4, and are stabilized by Van der Waals' interactions with surrounding amino acid residues. Compound **8a** was found to inhibit tubulin polymerization *in vitro* with an IC_{50} value of 1.7 μM. The potent cytotoxicity of these novel compounds and their inhibition of tubulin dynamics make these triazole analogues promising candidates for development as anti-cancer drugs.

Introduction

The combretastatins (Fig. 1, **1** and **2**) were first isolated from the South African bush willow tree *Combretum caffrum*, of which *cis*-combretastatin A-4 (*cis*-CA-4, **1**) is the major component.[1] Three analogues of combretastatin *cis*-CA-4: CA-4P (**3**), Oxi4503 (**4**) and AVE8062 (**5**) (Fig. 1) are currently in clinical trials for treatment of a variety of cancers, and have improved water solubility, cytotoxicity, efficacy and a better safety profile compared to *cis*-CA-4.[2-5] These combretastatin analogues are also known to be vascular disrupting agents (VDAs) and have proven to be advantageous cytotoxic agents, since they target the tumor vasculature causing hemorrhagic necrosis and cell death.[6]

The CA-4 analogues are generally classified as tubulin polymerization inhibitors with an anti-mitotic mechanism of action, due to their ability to disrupt microtubule dynamics and hence mitotic spindle formation by binding to the same site as colchicine on tubulin dimers.[7, 8] These small molecule VDAs also induce hypoxia-driven necrosis of solid tumors, and are able to induce apoptosis by cell-cycle arrest.[9, 10]

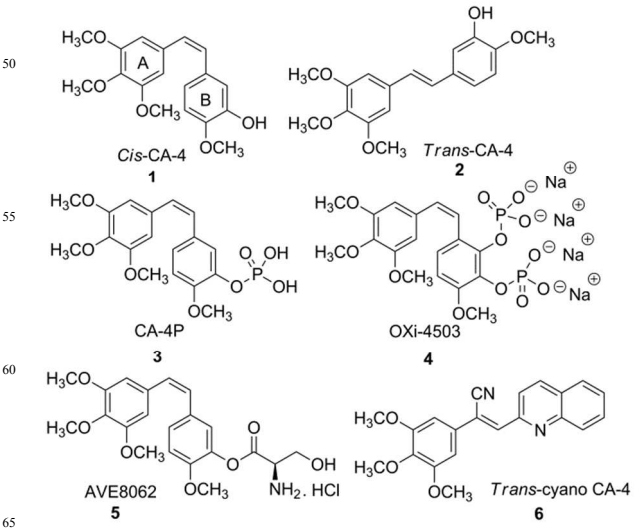

Fig 1. Chemical structures of *cis*-CA-4 (**1**) and its derivatives (**2**-**6**).

CA-4 analogues are highly cytotoxic against human cancer cell lines. CA4-P (**3**) exhibits potent cytotoxicity against anaplastic thyroid cancer cells lines,[11] and Oxi-4503 (**4**) is a potent anti-leukemic compound.[12] AVE8062 (**5**) is an effective cytotoxic agent against head and neck squamous cell carcinoma,[13] including multidrug resistant forms of this cell line.[14] Tron *et al.* have reported that the *cis*-configured double bond of *cis*-CA-4, with a 3,4,5-trimethoxyphenyl ring (Ring A) on one side and a 4-methoxysubstituted phenyl ring on the

[a]*Department of Pharmaceutical Sciences, College of Pharmacy, University of Arkansas for Medical Sciences, Little Rock, AR 72205, USA* [c] *Department of Biochemistry and Molecular Biology, University of Arkansas for Medical Sciences, Little Rock, AR 72205-7199, U.S.A.* ∗ *Corresponding author: Tel.: +1-501-686-6495; fax: +1-501-686-6057; e-mail: pacrooks@uams.edu*

other side (Ring B), is an essential structural moiety for optimal cytotoxic activity in *cis*-CA-4 analogues.[15-17] Recently, we have investigated the anticancer activities of a series of *trans*-cyano-CA-4 analogs in which replacement of ring B with different heterocycles, such as quinoline (**6**), benzothiophene (**7a-f** and **10a-c**), benzofuran (**7g-h**) and indole (**7i** and **10d-e**), has occurred; we have determined the effect of these structural changes on anticancer activity.[18, 19] We have also evaluated the effects of structurally modifying ring A by introducing differently substituted methoxy and hydroxy moieties into this phenyl ring.[18]

The isomerization of the *cis*-configured CA-4 analogues to their *trans*-forms in solution is one of the major disadvantages of these molecules. In this respect, we have shown that isomerization of *trans*-cyano CA-4 analogues to their *cis*-cyano CA-4 forms is also observed in solution.[18] To restrict *cis-trans* isomerization in these CA-4 analogues, different heterocylic ring systems, such as doxolane,[20] thiazole[21] 1,5-disubstituted 1,2,3-triazoles,[22-26] 1,2,4-triazoles[27, 28] and imidazole,[29] have been incorporated into the stilbene double bond.

In the present report, we have prepared a series of stable analogues of *cis*-cyano CA-4 by constructing a triazole ring system across the olefinic bond between aromatic rings A and B. This (2*H*)-1,2,3-triazole heterocyclic bridge unit was established by chemical modification of existing *trans*-cyano CA-4 analogues via [3+2] cycloaddition of azide ion across the double bond. This novel and simple structural modification led to an improvement in the stability and biological properties of these new CA-4 analogues. We now report on the synthesis and *in vitro* anti-cancer activities of a variety of 4-heteroaryl-5-aryl-(2*H*)-1,2,3-triazole CA-4 analogues, and their ability to inhibit tubulin polymerization *in vitro*. Some of the analogues were also tested for cytotoxicity against Hs578T breast cancer cell lines. In addition, molecular modeling studies of the most active inhibitors indicate that they interact with the colchicine binding site on α,β-tubulin, and this has been confirmed in *in vitro* tubulin polymerization inhibition studies.

Chemistry

The formation of the 1,2,3-triazole ring system is well known in the literature as a "click chemistry" product from a thermally induced Cu(I)-catalyzed (CuAAC) Huisgen [3+2]cycloaddition azide-alkyne reaction.[30] The click chemistry approach is widely used in the synthesis and regioisomeric formation of 1,4-disubstituted-1,2,3-triazoles in the presence of CuAAC in excellent yields.[31-34] The regioisomeric synthesis of 1,5-disubstituted-1,2,3-triazoles has also been reported with high selectivity utilizing different metal ions in magnesium-, cerium- and ruthenium-mediated reactions.[35-37]

We have recently reported the synthesis of a wide variety of 4,5-disubstitued-1,2,3-(1*H)*-triazole analogues.[38, 39] We used a two stage synthesis, i.e. the preparation of the precursor *trans*-cyano-CA-4 analogue, which utilizes our previously published procedure,[18] followed by synthesis of the target (*2H*)-1,2,3-triazole CA-4 compounds **8a-8i** and **11a-11e** by reaction of the *trans*-cyano CA-4 analogue with sodium azide in DMSO at 100 ^{o}C over 1-6 hrs utilizing L-proline as a Lewis base. The desired (*2H*)-1,2,3-triazole products were obtained in 75-96% yield[38] (Schemes 1 and 2) (Note: the use of *cis*-cyano CA-4 analogues in the above reaction led to lower yields of the triazole product[39]). The *N*-2 methylated analogue **9** was prepared from the reaction of **8a** with methyl iodide/K_2CO_3 in acetone (Scheme 2). Confirmation of the structure and purity of these analogues is reported elsewhere, and was obtained from single crystal X-ray diffraction studies,[40] and ^{1}H-NMR, ^{13}C-NMR and high resolution mass spectroscopic analysis.[38]

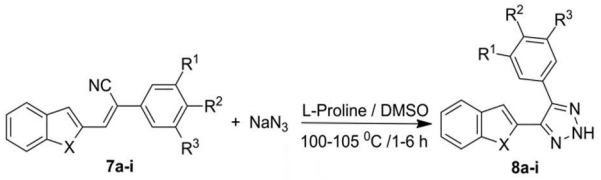

7a-i 8a-i

Entry	X	R^1	R^2	R^3
8a	S	OCH_3	OCH_3	OCH_3
8b	S	OCH_3	H	OCH_3
8c	S	H	OCH_3	H
8d	S	OH	OCH_3	H
8e	S	3,4-methylenedioxy		H
8f	S	H	SCH_3	H
8g	O	OCH_3	OCH_3	OCH_3
8h	O	OCH_3	H	OCH_3
8i	NH	OCH_3	OCH_3	OCH_3

Scheme 1 Synthesis of substituted 4-heteroaryl-2-yl-5-phenyl-2*H*-1,2,3-triazoles (**8a-i**).

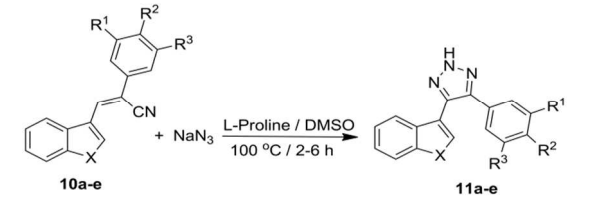

10a-e 11a-e

Entry	X	R^1	R^2	R^3
11a	S	OCH_3	OCH_3	OCH_3
11b	S	OCH_3	OCH_3	H
11c	S	H	OCH_3	H
11d	NH	OCH_3	OCH_3	OCH_3
11e	NH	OCH_3	H	OCH_3

Scheme 2 Synthesis of substituted 4-heteroaryl-3-yl-5-phenyl-2*H*-1,2,3-triazoles (**11a-e**).

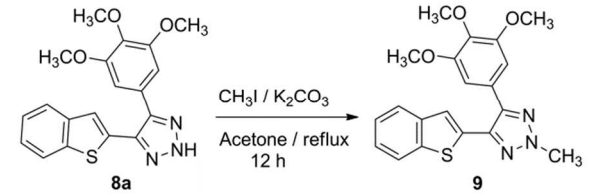

8a 9

Scheme 3 Synthesis of 4-(benzo [*b*]thiophen-2-yl)-2-methyl-5-(3,4,5-trimethoxyphenyl)-2*H*-1,2,3-(2*H)*-triazole (**9**).

Biological Evaluation

A. *In vitro* growth inhibition and cytotoxicity

The above triazole analogues were evaluated for their anticancer activities against a panel of 60 human cancer cell lines, which incorporates different subpanels representing leukemia, non-small cell lung, colon, central nervous system, melanoma, ovary, renal, prostate, and breast cancer cell lines, at a concentration of 10^{-5} M utilizing the procedure described by Rubinstein et al.[41] Compounds that showed 60% growth inhibition in at least eight of the 60 cell lines screened were further evaluated in a five-dose screen.

From the preliminary screen, compounds **8a**, **11b**, **11d**, **11e** and **9** were selected for five-dose studies and their GI_{50} values determined (Table 1). GI_{50} values represent the molar drug concentration required to cause 50% growth inhibition. In the five-dose studies, 5 different concentrations at 10-fold dilutions (10^{-4} M, 10^{-5} M, 10^{-6} M, 10^{-7} M and 10^{-8} M) were utilized and incubations were carried out over 48 h exposure to drug. Compounds **8a**, **11b**, **11d**, **11e** and **9** exhibited GI_{50} values in the low nanomolar range against all 60 human cancer cell lines in the panel. The results are presented in Table 1.

Compound **8a** (4-(benzo[*b*]thiophen-2-yl)-5-(3,4,5-trimethoxyphenyl)-2*H*-1,2,3-triazole) exhibited GI_{50} values <0.050 μM in all the 60 human cancer cell lines in the panel, and had GI_{50} <0.01 μM in 80% of the cancer cells in the panel (Table 1). Compound **8a** exhibited particularly potent growth inhibition properties against all six cell lines in the breast cancer subpanel, with GI_{50} values of <0.01 μM to 0.014 μM.

Compound **9**, obtained by *N*-methylation of **8a,** exhibited GI_{50} values ranging from 0.023 μM to 0.744 μM in 84% of the cancer cell lines screened and showed moderate growth inhibition properties in all six breast cancer cell lines, with GI_{50} values in the range of 0.040 μM to 1.6 μM (except for the T-47D cell line). This compound also exhibited potent growth inhibition against NCI-H522 lung cancer (GI_{50} = 0.023 μM) and MDA-MB-435 melanoma (GI_{50} = 0.025 μM) cell lines (Table 1).

Compound **11b** exhibited GI_{50} values ranging from 0.337 μM to 13.3 μM against the entire 60 cancer cell panel screened, and showed moderate growth inhibition properties against all six breast cancer cell lines, with GI_{50} values in the range of 0.63 μM to 3.21 μM. This compound exhibited potent growth inhibition against MDA-MB-435 melanoma cells (GI_{50} = 0.337 μM) (Table 1).

Compound **11d** exhibited GI_{50} values ranging from 0.014 μM to 0.44 μM in 90% of the cancer cell lines screened and showed potent growth inhibition properties in all six breast cancer cell lines, with GI_{50} values in the range of 0.028 μM to 0.089 μM. This compound exhibited potent growth inhibition against MDA-MB-435 melanoma cells (GI_{50} = 0.014 μM) (Table 1). The average GI_{50} value of this compound against all the cancer cell lines screened was 0.424 μM.

Table 1. Antitumor activity (GI_{50} in μM)[a] data for compounds **8a**, **9**, **11b**, **11d**, **11e** in the NCI 60-cell line screen

Panel/cell line	8a	9	11b	11d	11e
	GI_{50} (μM)	GI_{50} (μM)	GI_{50} (μM)	GI_{50} (μM)	GI_{50} (μM)
Leukemia					
CCRF-CEM	0.028	0.22	3.29	0.048	0.037
HL-60(TB)	<0.01	0.048	1.70	0.046	0.033
K-562	<0.01	0.042	0.516	0.053	0.031
MOLT-4	0.042	0.333	3.05	0.16	0.063
RPMI-8226	<0.01	0.362	3.64	0.09	0.053
SR	<0.01	nd	nd	0.09	0.047
Lung Cancer					
A549/ATCC	0.023	0.167	4.52	0.09	0.088
EKVX	0.010	0.466	3.42	na	na
HOP-62	0.015	0.553	2.18	na	na
HOP-92	<0.01	0.080	0.921	nd	0.029
NCI-H226	nd	>100	13.2	0.39	0.075
NCI-H23	<0.01	0.392	3.94	0.27	0.124
NCI-H322M	<0.01	1.26	7.79	nd	40.7
NCI-H460	<0.01	0.069	3.56	0.042	0.038
NCI-H522	<0.01	0.023	0.601	0.021	0.013
Colon Cancer					
COLO 205	<0.01	0.082	2.82	0.034	0.035
HCC-2998	0.036	0.407	4.21	0.44	0.251
HCT-116	<0.01	0.073	2.84	0.041	0.031
HCT-15	<0.01	0.058	1.67	0.035	0.031
HT29	0.020	0.055	2.78	0.033	0.031
KM12	0.022	0.054	2.28	0.045	0.045
SW-620	<0.01	0.063	3.09	0.043	0.035
CNS Cancer					
SF-268	<0.01	0.63	3.69	0.071	0.067
SF-295	<0.01	0.036	2.33	0.032	0.026
SF-539	<0.01	0.149	1.84	0.031	0.024
SNB-19	<0.01	0.254	4.67	0.061	0.056
SNB-75	<0.01	nd	nd	0.030	0.025
U251	<0.01	0.078	2.19	0.059	0.054
Melanoma					
LOX IMVI	<0.01	0.168	3.04	0.071	0.055
MALME-3M	nd	16.9	13.3	nd	nd
M14	<0.01	0.076	1.95	0.036	0.031
MDA-MB-435	<0.01	0.025	0.337	0.014	0.010
SK-MEL-2	<0.01	0.059	1.44	0.030	0.031
SK-MEL-28	<0.01	13.0	4.63	0.112	Nd
SK-MEL-5	<0.01	0.225	2.83	0.043	0.034
UACC-257	<0.01	51.6	10.9	13.9	>100.0
UACC-62	<0.01	0.053	2.77	0.043	0.034
Ovarian Cancer					
IGROV1	<0.01	0.707	4.21	na	na
OVCAR-3	<0.01	0.354	1.94	0.033	0.028
OVCAR-4	0.042	nd	6.33	1.16	2.67
OVCAR-5	0.042	2.36	7.91	0.381	0.416
OVCAR-8	<0.01	0.352	4.24	1.16	0.070
NCI/ADR-RES	<0.01	0.103	2.39	0.034	0.030
SK-OV-3	<0.01	0.311	2.37	0.042	0.034
Renal Cancer					
786-0	<0.01	0.312	3.26	0.035	0.030
A498	<0.01	0.041	2.96	0.035	0.033
ACHN	<0.01	0.294	3.94	0.043	0.045
CAKI-1	<0.01	3.77	3.69	0.044	0.038
RXF 393	nd	0.286	2.11	0.164	0.052
SN12C	0.048	nd	8.80	1.39	0.069
TK-10	nd	0.578	2.98	1.39	0.083
UO-31	<0.01	0.744	2.78	0.087	0.062
Prostate Cancer					
PC-3	0.034	0.077	3.08	0.044	0.038
DU-145	<0.01	0.263	3.77	0.090	0.075
Breast Cancer					
MCF7	<0.01	0.040	1.45	0.029	0.029

MDA-MB-	0.014	1.60	3.21	0.089	0.076
HS 578T	<0.01	0.270	2.25	0.042	0.031
BT-549	<0.01	0.422	2.17	0.028	0.017
T-47D	nd	>100	2.83	0.048	0.044
MDA-MB-468	<0.01	0.082	0.63	0.042	0.037

na: not analyzed; nd: not determined; [a]GI_{50}: 50% growth inhibition, concentration of drug resulting in a 50% reduction in net cell growth as compared to cell numbers on day 0.

Compound **11e** exhibited GI_{50} values ranging from 0.01 μM to 41.6 μM in 94% of the cancer cell lines screened and showed potent growth inhibition properties in all six breast cancer cell lines, with GI_{50} values in the range of 0.017 μM to 0.076 μM. This compound exhibited potent growth inhibition against MDA-MB-435 melanoma cells (GI_{50} = 0.01 μM) and NCI-H522 (GI_{50} = 0.013 μM) non-small cell lung cancer cell lines (Table 1). The average GI_{50} value of this compound against all 60 cancer cell lines screened was 0.856 μM.

B. Cytotoxic effects of 8a, 8b, and 8g on Hs578T breast cancer cell lines

Compound **8a** and its analogues (**8b** and **8g**) were tested for cytotoxicity against the triple negative breast cancer (TNBC)-derived Hs578T cell line. The GI_{50} estimates for compounds **8a**, **8b**, and **8g** were all below 100 nM (Fig. 2). However, the potency of compound **8a** remained two- to six-fold greater than either **8b** or **8g**. Comparing the results for **8a**, **8b** and **8g** revealed that replacing the 3,4,5-trimethoxyphenyl moiety of **8a** with a 3,5-dimethoxyphenyl group to afford **8b**, results in a more pronounced effect on cytotoxicity than replacing the benzothiophen-2-yl moiety with a benzofuran-2-yl group (**8g**).

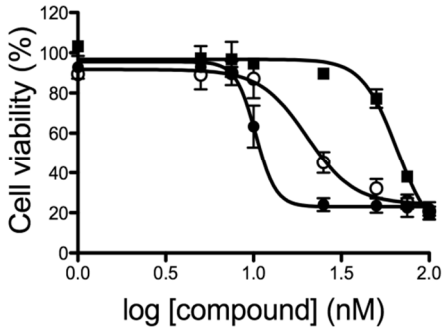

Fig. 2 Hs578T TNBC cell viability is sensitive to compounds **8a**, **8b**, and **8g**. Dose-response curves for Hs578T cell viability in the presence of varying concentrations of compounds **8a** (closed circles), **8b** (closed squares), and **8g** (open circles) are shown. The values shown represent the mean ± s.d. (n=3). Fitting the data to a variable slope log (inhibitor) vs. response equation yields the following GI_{50} estimates (with 95% confidence intervals): **8a**: GI_{50} = 10 (9.8-11) nM, **8b**: GI_{50} = 65 (52-82) nM, **8g**: GI_{50} = 20 (16- 26) nM.

C. Molecular modeling studies

Molecular modeling studies were performed for four active (2*H*)-1,2,3-triazoles analogues (**8a**, **8g**, **11d**, and **11e**) using SYBYL-X 2.1. Binding interactions of these triazole analogues were studied by docking them at the colchicine-binding site on tubulin. 3-D coordinates for the tubulin-colchicine complex were obtained from the RSCB protein data bank (pdb id: 4O2B). For preparation of tubulin to perform the docking calculations, the geometry of the protein molecule was optimized using energy minimization techniques after the addition of hydrogen atoms. Since no structured water molecule was present in the binding pocket, all the water molecules in the protein were deleted during the preparation of structure for docking calculations. Amino acid side chain bumps were fixed and terminal amino acid were charged to mimic the biological environment. Hydrogen atoms were added to the structure. The Kollman force field was applied and the protein was minimized using the Powell method and Pullman charges. The triazole analogue structures were initially generated in 2-D format in Chem-Draw. For generating energy-minimized structures, the 2-D structures were converted to 3-D using ChemDraw3D and all the structures were saved in Mol2 format. The structures were imported to Sybyl in the Mol2 format. In SYBYL, TRIPOS force field was applied and 3-D structure coordinates were taken through a series of minimization processes. Firstly, all the structures we minimized using the BFGS method. Then, MOPAC charges were calculated for each molecule followed by another minimization step. Each molecule was then checked for charges, bond angle, torsion angles and geometry. All the molecules were saved in one directory and prepared for docking via the ligand preparation tool. For the docking analysis using the Surflex program, a protomol was generated at the colchicine-binding site in tubulin. This protomol is the representation of the binding site that simulates the binding environment experienced by the ligand. The docking analysis is performed using the Surflex Dock-Gemox module which lists the C-Scores (consolidated scores) for each molecule. The C-Score is a measure of the goodness of fit. The C-Score function combines the binding score obtained from five different scoring algorithms; namely: Total Score, G Score, PMF Score, D Score and Chem Score. In these docking calculations, the flexibilities of the ligands are accounted for by considering 20 different conformational states and scoring each of them.

Docking analysis at the colchicine binding site determined the binding modes of the four triazole analogues. Compound **8a** exhibited the strongest binding interactions at the colchicine binding site in tubulin compared to the other three analogues. **8a** participates in strong hydrogen bonding with ASN 258 and THR 353 (Fig. 3) and makes a weak hydrogen bond with ASN 258. Out of 20 different tested conformations of **8a**, four conformations showed the highest C-Score of 4, which was higher than any of the C-Scores for the other three triazole analogues. Compound **8g** is participates in hydrogen bonding with ASN 258 and ALA 317, with one conformation exhibiting the highest C-Score of 4. Compounds **11d** and **11e** each participate in a hydrogen bonding interaction with ASN 258, while **11d** participates in another hydrogen bonding interaction with THR 356, and **11e** makes hydrogen bond with ALA 317 (Fig. 3). ASN 258 hydrogen bond interactions are common in all four docked triazoles.

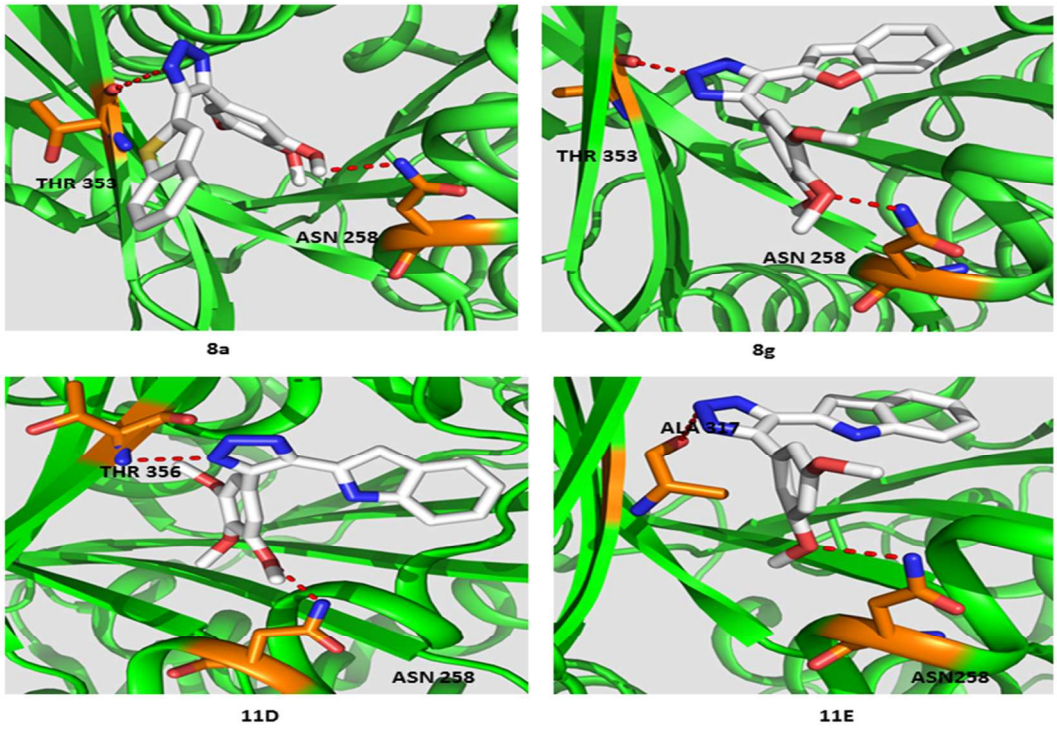

Fig. 3 Binding modes of compounds **8a**, **8g**, **11d** and **11e** at the colchicine binding site on tubulin

In summary, **8a** exhibited the strongest binding interactions with tubulin at the colchicine-binding site, which is consistent with the anticancer screening data (Table 1). Thus, the above molecular modeling data predicts that stable, more drug-like triazolo derivatives of the *cis*-cyano CA-4 analogues formed by constructing a heterocyclic ring system across the olefinic bond between aromatic rings A and B will retain the tubulin targeting properties of the parent compounds.

D. Inhibition of tubulin polymerization

The ability of compounds **8a**, **11d**, **11e** and **9** to inhibit tubulin polymerization was determined using a commercially available *in vitro* assay (Cytoskeleton Inc., Denver, CO). We examined the ability of three of the most active CA-4-(2*H*)-1,2,3-triazoles, **8a**, **11d**, and **11e**, to inhibit tubulin polymerization using an *in vitro* assay. Compound **8a**, which exhibited the greatest overall potency against the NCI 60 human cancer cell line panel, was found to inhibit tubulin polymerization with an IC_{50} value of 1.7 (± 0.4) μM (Fig. 4), where the reported values represent the mean ± s.d. (n=3). Compounds **11d** and **11e** inhibited tubulin polymerization with IC_{50} values of 18.5 (± 9.8) μM and 13.5 (± 3.5) μM, respectively, in this assay. The *N*-methylated analogue **9** failed to inhibit tubulin polymerization even at concentrations as high as 200 μM (data not shown). These results are consistent with the idea that compound **8a** exerts some of its cytotoxic effects on cells through inhibition of tubulin polymerization. The less potent inhibition of tubulin polymerization by compounds **11d** and **11e** is consistent with the general trend towards decreasing potency (but still significant), as determined from GI_{50} values from the cancer cell screens, when compared to compound **8a**, and is also consistent with the molecular docking studies. However, based on the *in vitro* assay results, it would appear that the cytotoxic effects of compound **9** observed in cell culture are not mediated by inhibition of tubulin polymerization, but are instead the result of an unknown mechanism of action.

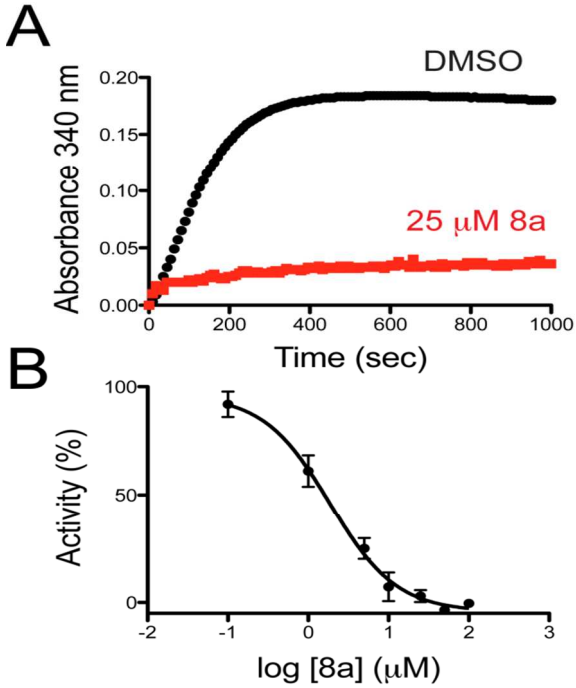

Fig. 4 Compound **8a** inhibits tubulin polymerization. (A) An *in vitro* assay was used to measure inhibition of tubulin polymerization by compound **8a**. (B) A dose-response curve for tubulin polymerization in the presence of varying concentrations of compound **8a**. The values shown represent the mean ± s.d. (n=3).

Conclusions

We have evaluated a small library of novel 4-heteroaryl-5-aryl-(2*H*)-1,2,3-triazoles that are structurally related to *trans*-cyano CA-4 analogues that inhibit tubulin polymerization. These compounds have been evaluated in a panel of 60 human cancer cell lines for their anti-cancer activities, and in assays to determine their ability to inhibit tubulin polymerization. The most potent compound, **8a**, and two closely related analogues, **8b** and **8g**, were also tested for cytotoxicity against triple negative Hs578T breast cancer cell lines. Compound **8a**, a benzothiophen-2-yl derivative was shown to be a more potent anti-cancer agent than its isosteric indol-2-yl (**8i**) and benzofuran-2-yl (**8g**) congeners. Compound **8a** was also found to be the most effective inhibitor of tubulin polymerization. However, the benzothiophen-3-yl isostere of **8a**, compound **11a**, did not possess any significant anti-cancer activity, although indol-3-yl analogues that incorporate a 3,4,5-trimethoxyphenyl (**11d**) or a 3,5-dimethoxyphenyl (**11e**) moiety into their structure were potent anti-cancer agents. Interestingly, a significant decrease in anti-cancer activity was observed with the *N*-2-methylated analogue **9** when compared to the parent compound **8a**.

In summary, the anti-cancer screening data, inhibition of tubulin polymerization, and molecular docking studies are all promising indicators that compound **8a** warrants further study as a potential anti-cancer agent.

EXPERIMENTAL PROCEDURES

General synthetic procedure for the synthesis of 4-heteroaryl-5-(substituted phenyl)-2H-1,2,3-triazoles (8a-i and 11a-e):[25] Sodium azide (0.01 mol) in DMSO (1 ml) was added to the appropriate heteroaryl cyanostilbene (0.01 mol) followed by addition of L-proline (0.002 mol). The resulting reaction mixture was heated to 100 °C and stirred for 1-6 h. After completion of the reaction, the reaction mixture was cooled to 20 ^{o}C, water (10 ml) was added, and the resulting slurry was extracted with ethyl acetate (2x10 ml). The organic layers were separated and combined, dried over anhydrous sodium sulphate, concentrated on a rotovaporator and purified by silica gel column chromatography (ethylacetate:hexanes 1:4) to afford the pure product.

Synthetic procedure for the synthesis of *4-(benzo[b] thiophen-2-yl)-2-methyl-5-(3,4,5-trimethoxyphenyl)-2H-1,2,3-triazole (9):*[25] A mixture of 4-(benzo[*b*]thiophen-2-yl)-5-(3,4,5-trimethoxy phenyl)-2*H*-1,2,3-triazole (**6a**) (1 mmol), K_2CO_3 (10 mmol) and MeI (2 mmol) in 10 volumes of acetone was refluxed for 8 h and the reaction monitored by TLC analysis. After completion, the reaction mixture was filtered to remove the K_2CO_3, washed with acetone and the filtrate evaporated to dryness on a rotovaporator. The resulting residue was submitted to ethyl acetate/hexane flash column chromatography to yield 4-(benzo[*b*]thiophen-2-yl)-2-methyl-5-(3,4,5-tri methoxyphenyl)-2*H*-1,2,3-triazole (**9**) as a light yellow solid.

***NCI-60 cell line anti-cancer screening assay*:** All the synthesized molecules were evaluated for their anti-cancer activity in a preliminary screen against a panel of 60 human cancer cell lines (NCI-60 panel) at a concentration of 10^{-5} M utilizing the procedure described by Rubinstein et al.[41] In this cellular assay the growth inhibition of the test compounds is measured by determining percentage cell growth (PG) inhibition. Optical density (OD) measurements of sulforhodamine B (SRB)-derived colour, just before exposing the cells to the test compound (ODt_{zero}), and after 48 h exposure to the test compound (OD_{test}) or the control vehicle (OD_{ctrl}) is recorded. The growth percentage compared to control is calculated utilizing the reported protocols.[42] From the preliminary screening potent compounds were further evaluated for five dose studies designed to determine GI_{50} values, which represent the molar drug concentration required for 50% cell growth inhibition. The compounds were dissolved in dimethyl sulfoxide (DMSO)/H_2O and evaluated using five different concentrations at 10-fold dilutions (10^{-4} M, 10^{-5} M, 10^{-6} M, 10^{-7} M and 10^{-8} M) following 48 hr of incubation.

***Screening against breast cancer cell lines (Hs578T) assay*:** Hs578T cells were seeded at 3,000 cells per well into 96-well plates and incubated overnight at 37 °C in DMEM containing 10% (v/v) FBS medium. The following day, various concentrations of triazole CA-4 analogues, or vehicle, were added to each plate and the plates were then incubated for an additional 48 hr. Cells were washed twice with Dulbecco's phosphate-buffered saline (DPBS, pH 7.4) and incubated with 2 μM Calcein-AM for 30 min at 25 °C. Fluorescence was measured using a 490 nm excitation wavelength and monitoring emission at 520 nm. The fluorescence intensity is proportional to the number of viable cells. The fluorescence intensity of control (untreated) cells was taken as 100% viability, and the relative cell viability compared to control was calculated.

***Inhibition of tubulin polymerization assay*:** The tubulin polymerization was performed in 80 mM PIPES (pH 6.9) buffer containing 2 mM $MgCl_2$, 0.5 mM EGTA, 100 mM GTP, and 10% (v/v) glycerol. The assay buffer was prepared on ice immediately prior to performing the tubulin polymerization experiments in order to minimize GTP hydrolysis. Tubulin (4 mg) was reconstituted in 1 mL of cold assay buffer for a final concentration of 4 mg/mL. The reconstituted tubulin was placed on ice for a minimum of 3 minutes prior to starting the experiment. Compounds were dissolved in 50% (v/v) DMSO/dH_2O solution. The 96-well plate was pre-warmed to 37 °C for 30 minutes in a Synergy4 plate reader (BioTek, Winooski, VT). Compound (10x of final concentration) or DMSO control (4 μL) was added to the plate and incubated for 2 minutes at 37 °C. Cold tubulin (36 μL of 4 mg/mL) was added to each well and polymerization was initiated by placing the plate at 37 °C. Polymerization was measured over time by monitoring the change in absorbance at 340 nm. The initial portion of the reaction was fit to a linear equation and the slope was used to estimate the rate of tubulin polymerization. The rate of polymerization in the presence of triazole analogue was

normalized against the control reaction and percent activity was plotted against the log of the inhibitor concentration. The IC_{50} values for test compounds were calculated using a variable slope dose-response curve.

Acknowledgments

We are grateful to NCI/NIH (Grant Number CA 140409 to P.A.C. and CA 183895 to R.L.E.) and to the Arkansas Research Alliance (ARA) for financial support and to the NCI Developmental Therapeutic Program (DTP) for screening data.

References

1 G. R. Pettit, G. M. Cragg, D. L. Herald, J. M. Schmidt, P. Lobavanijaya, *Can. J. Chem*, 1982, **60**, 1374-1376.
2 T. M. Beale, P. J. Bond, J. D. Brenton, D. S. Charnock-Jones, S. V. Ley and R. M. Myers, *Bioorg. Med. Chem.*, 2012, **20**, 1749-1759.
3 P. Nathan, M. Zweifel, A. R. Padhani, D. M. Koh, M. Ng, D. J. Collins, A. Harris, C. Carden, J. Smythe, N. Fisher, N. J. Taylor, J. J. Stirling, S. P. Lu, M. O. Leach, G. J. Rustin and I. Judson, *Clin. Cancer Res.*, 2012, **18**, 3428-3439.
4 E. I. Zimmerman, D. C. Turner, J. Buaboonnam, S. Hu, S. Orwick, M. S. Roberts, L. J. Janke, A. Ramachandran, C. F. Stewart, H. Inaba and S. D. Baker, *Blood*, 2013, **122**, 3607-3615.
5 J. V. Pawel, V. Gorbounova, M. Reck, D. M. Kowalski, A. Allard, M. Chadjaa, A. Rey, J. Bennouna, F. Grossi and D. Investigators, *Lung Cancer*, 2014, **85**, 224-229.
6 G. Kremmidiotis, A. F. Leske, T. C. Lavranos, D. Beaumont, J. Gasic, A. Hall, M. O'Callaghan, C. A. Matthews and B. Flynn, *Mol. Cancer Ther.*, 2010, **9**, 1562-1573.
7 R. J. D'Amato, C. M. Lin, E. Flynn, J. Folkman and E. Hamel, *Proc. Natl. Acad. Sci. U. S. A.*, 1994, **91**, 3964-3968.
8 G. Kuznetsov, K. TenDyke, M. J. Towle, H. Cheng, J. Liu, J. P. Marsh, S. E. Schiller, M. R. Spyvee, H. Yang, B. M. Seletsky, C. J. Shaffer, V. Marceau, Y. Yao, E. M. Suh, S. Campagna, F. G. Fang, J. J. Kowalczyk and B. A. Littlefield, *Mol.Cancer Ther.*, 2009, **8**, 2852-2860.
9 R. Romagnoli, P. G. Baraldi, M. D. Carrion, C. Lopez Cara, D. Preti, F. Fruttarolo, M. G. Pavani, M. A. Tabrizi, M. Tolomeo, S. Grimaudo, A. Di Cristina, J. Balzarini, J. A. Hadfield, A. Brancale and E. Hamel, *J. Med. Chem.*, 2007, **50**, 2273-2277.
10 G. M. Tozer, C. Kanthou and B. C. Baguley, *Nat. Rev. Cancer*, 2005, **5**, 423-435.
11 J. A. Sosa, J. Balkissoon, S. P. Lu, P. Langecker, R. Elisei, B. Jarzab, C. S. Bal, S. Marur, A. Gramza and F. Ondrey, *Surgery*, 2012, **152**, 1078-1087.
12 G. J. Madlambayan, A. M. Meacham, K. Hosaka, S. Mir, M. Jorgensen, E. W. Scott, D. W. Siemann and C. R. Cogle, *Blood*, 2010, **116**, 1539-1547.
13 C. Clemenson, E. Jouannot, A. Merino-Trigo, C. Rubin-Carrez and E. Deutsch, *Invest. New Drugs*, 2013, **31**, 273-284.
14 H. Nakamura, H. Kuroda, H. Saito, R. Suzuki, T. Yamori, K. Maruyama and T. Haga, *Chem. Med. Chem*, 2006, **1**, 729-740.
15 G. C. Tron, T. Pirali, G. Sorba, F. Pagliai, S. Busacca and A. A. Genazzani, *J. Med. Chem.*, 2006, **49**, 3033-3044.
16 H. P. Hsieh, J. P. Liou and N. Mahindroo, *Curr. Pharm. Des.*, 2005, **11**, 1655-1677.
17 A. Cirla and J. Mann, *Nat. Prod. Rep.*, 2003, **20**, 558-564.
18 N. R. Penthala, V. N. Sonar, J. Horn, M. Leggas, J. S. Yadlapalli and P. A. Crooks, *Med. Chem. Comm.*, 2013, **4**, 1073-1078.
19 N. R. Penthala, V. Janganati, S. Bommagani and P. A. Crooks, *Med. Chem. Comm.*, 2014, **5**, 886-890.
20 R. Shirai, H. Takayama, A. Nishikawa, Y. Koiso and Y. Hashimoto, *Bioorg. Med. Chem. Lett.*, 1998, **8**, 1997-2000.
21 K. Ohsumi, T. Hatanaka, K. Fujita, R. Nakagawa, Y. Fukuda, Y. Nihei, Y. Suga, Y. Morinaga, Y. Akiyama and T. Tsuji, *Bioorg. Med. Chem. Lett.*, 1998, **8**, 3153-3158.
22 K. Odlo, J. Hentzen, J. F. dit Chabert, S. Ducki, O. A. Gani, I. Sylte, M. Skrede, V. A. Florenes and T. V. Hansen, *Bioorg. Med. Chem.* 2008, **16**, 4829-4838.
23 C. Vilanova, S. Torijano-Gutierrez, S. Diaz-Oltra, J. Murga, E. Falomir, M. Carda and J. Alberto Marco, *Eur. J. Med. Chem.*, 2014, **87**, 125-130.
24 O. W. Akselsen, K. Odlo, J. J. Cheng, G. Maccari, M. Botta and T. V. Hansen, *Bioorg. Med. Chem.* 2012, **20**, 234-242.
25 K. Odlo, J. Fournier-Dit-Chabert, S. Ducki, O. A. Gani, I. Sylte and T. V. Hansen, *Bioorg. Med. Chem.* 2010, **18**, 6874-6885.
26 D. V. Demchuk, A. V. Samet, N. B. Chernysheva, V. I. Ushkarov, G. A. Stashina, L. D. Konyushkin, M. M. Raihstat, S. I. Firgang, A. A. Philchenkov, M. P. Zavelevich, L. M. Kuiava, V. F. Chekhun, D. Y. Blokhin, A. S. Kiselyov, M. N. Semenova and V. V. Semenov, *Bioorg. Med. Chem.* 2014, **22**, 738-755.
27 Q. Zhang, Y. Peng, X. I. Wang, S. M. Keenan, S. Arora and W. J. Welsh, *J. Med. Chem.*, 2007, **50**, 749-754.
28 R. Romagnoli, P. G. Baraldi, O. Cruz-Lopez, C. Lopez Cara, M. D. Carrion, A. Brancale, E. Hamel, L. Chen, R. Bortolozzi, G. Basso and G. Viola, *J. Med. Chem.*, 2010, **53**, 4248-4258.
29 L. Wang, K. W. Woods, Q. Li, K. J. Barr, R. W. McCroskey, S. M. Hannick, L. Gherke, R. B. Credo, Y. H. Hui, K. Marsh, R. Warner, J. Y. Lee, N. Zielinski-Mozng, D. Frost, S. H. Rosenberg and H. L. Sham, *J. Med. Chem.*, 2002, **45**, 1697-1711.
30 R. Huisgen, G. Szeimies and L. Möbius, *Chem. Ber.*, 1967, **100**, 2494-2507.
31 V. V. Rostovtsev, L. G. Green, V. V. Fokin and K. B. Sharpless, *Angew. Chem. Int. Ed.*, 2002, **41**, 2596-2599.
32 C. W. Tornoe, C. Christensen and M. Meldal, *J. Org. Chem.*, 2002, **67**, 3057-3064.
33 A. K. Feldman, B. Colasson and V. V. Fokin, *Org. Lett.*, 2004, **6**, 3897-3899.
34 D. B. Ramachary, A. B. Shashank and S. Karthik, *Angew. Chem. Int. Ed. Engl.*, 2014, **53**, 10420-10424.
35 A. Krasinski, V. V. Fokin and K. B. Sharpless, *Org. Lett.*, 2004, **6**, 1237-1240.
36 L. Zhang, X. Chen, P. Xue, H. H. Sun, I. D. Williams, K. B. Sharpless, V. V. Fokin and G. Jia, *J. Am. Chem. Soc.*, 2005, **127**, 15998-15999.
37 Y. C. Wang, Y. Y. Xie, H. E. Qu, H. S. Wang, Y. M. Pan and F. P. Huang, *J. Org. Chem.*, 2014, **79**, 4463-4469.
38 N. R. Penthala, N. R. Madadi, V. Janganati and P. A. Crooks, *Tetrahedron Lett.*, 2014, **55**, 5562-5565.
39 N. R. Madadi, N. R. Penthala, L. Song, H. P. Hendrickson and P. A. Crooks, *Tetrahedron lett.*, 2014, **55**, 4207-4211.
40 N. R. Penthala, N. R. Madadi, S. Bommagani, S. Parkin and P. A. Crooks, *Acta Crystallogr. Sect. E: Struct. Rep. Online*, 2014, **70**, 392-395.
41 L. V. Rubinstein, R. H. Shoemaker, K. D. Paull, R. M. Simon, S. Tosini, P. Skehan, D. A. Scudiero, A. Monks and M. R. Boyd, *J. Natl. Canc. Inst.*, 1990, **82**, 1113-1118.
42 N. R. Madadi, N. R. Penthala, V. Janganati and P. A. Crooks, *Bioorg. Med. Chem. Lett.*, 2014, **24,** 601-603.

Graphical Abstract

Synthesis and anti-cancer screening of novel heterocyclic-(2*H*)-1,2,3-triazoles as potential anticancer agents

Narsimha Reddy Penthala, Leena Madhukuri, Shraddha Takkar, Nikhil Reddy Madadi, Gauri Lamture, Robert L. Eoff and Peter A. Crooks

Novel, stable combretastatin-A4 heterocyclic (2*H*)-1,2,3-triazole analogues displayed potent cytotoxic activity against both hematological and solid tumor cell lines with GI_{50} values in the low nanomolar range.

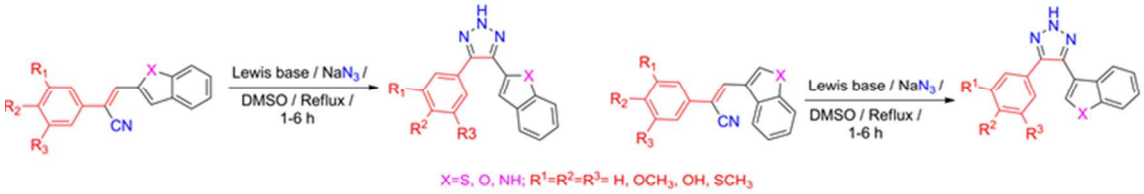

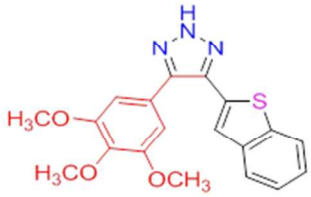

GI_{50} < 10 nM in 81% of the cancer cells in NCI-60 cancer cell lines

GI_{50} = 10.0 nM against Hs578T TNBC cells

IC_{50} = 1.7 μM against tubulin polymerization